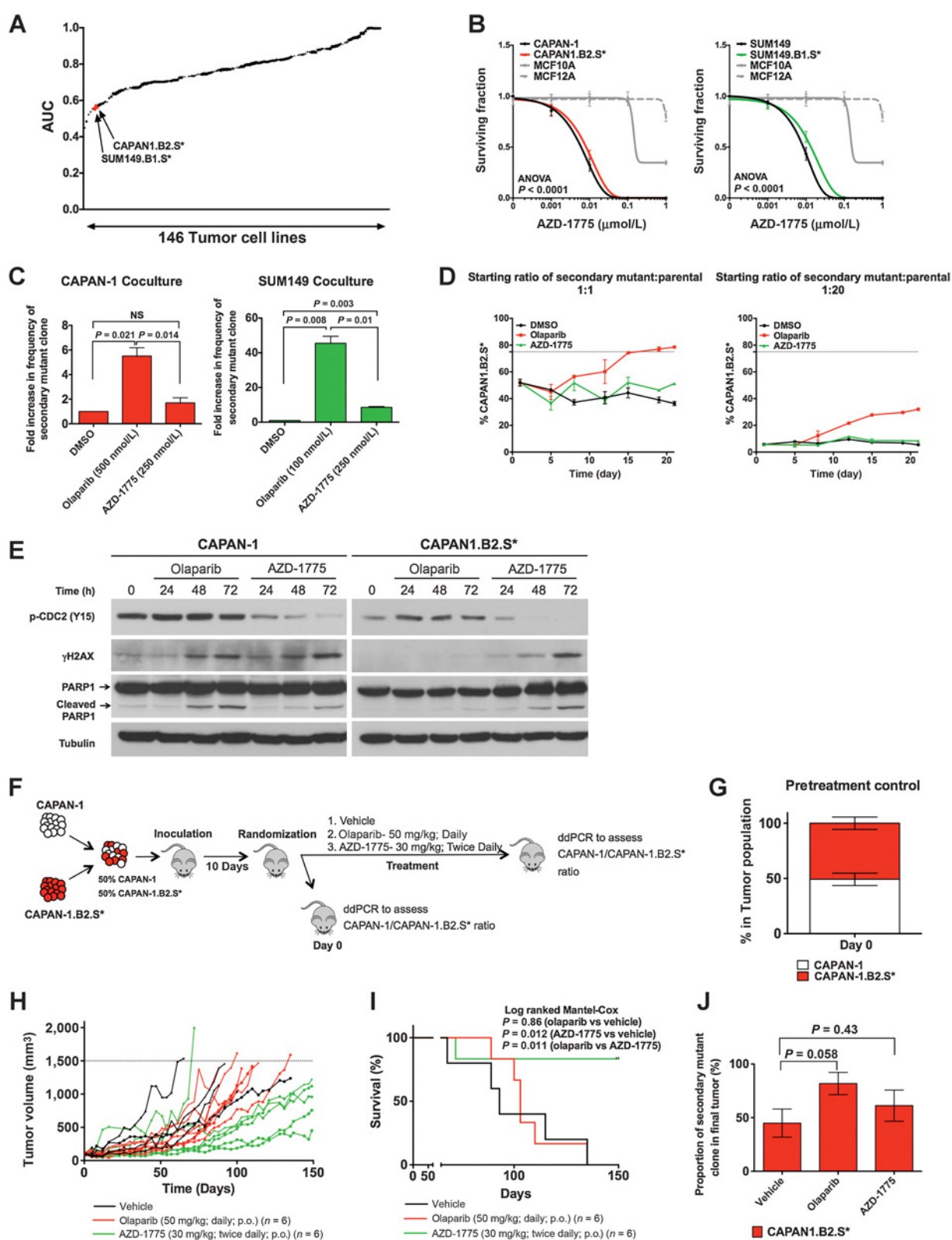


Dréan et al.

**Figure 5.**

PARP1-resistant, secondary mutant clones and parental tumor cells are sensitive to AZD-1775 *in vitro* and *in vivo*. **A**, Waterfall plot comparing AUC values collated from a 5-day exposure to AZD-1775 from 146 cancer cell lines. **B**, Dose-response survival curves illustrating 6-well clonogenic survival data in CAPAN1, CAPAN1.B2.S*, SUM149, SUM149.B1.S*, MCF-10A, and MCF-12A cells exposed to AZD-1775. **C**, Bar graph illustrating (Continued on the following page.)

marker to enable detection and monitoring of coculture populations via FACS (Supplementary Fig. S5A). We found that in the absence of drug exposure, the DLD1.*BRCA2*^{WT/WT} cells exhibited a selective advantage over DLD1.*BRCA2*^{-/-} cells, as previously shown (ref. 29; Supplementary Fig. S5B), and that these cells exhibit more than a 10-fold difference in olaparib sensitivity (Fig. 3A). We then mixed DLD1.*BRCA2*^{WT/WT} cells into DLD1.*BRCA2*^{-/-} cells *in vitro* at starting ratios of 1:1, 1:10, 1:100, and 1:1,000, exposed these cocultures to either olaparib or talazoparib, and monitored the temporal evolution of the population in response to PARPi (Supplementary Fig. S5A). Similar to the CAPAN1 and SUM149 isogenic models, we observed that olaparib and talazoparib both selected for DLD1.*BRCA2*^{WT/WT} cells over DLD1.*BRCA2*^{-/-} cells in a Darwinian fashion (Fig. 3B). For example, both olaparib and talazoparib exposure resulted in a 3-fold increase in DLD1.*BRCA2*^{WT/WT} cells compared with the DMSO-exposed cell population after 13 days of drug exposure (Fig. 3B). In addition, we noticed that the time taken for the DLD1.*BRCA2*^{WT/WT} clone to reach clonal dominance was less in cell populations that had higher starting proportion of DLD1.*BRCA2*^{WT/WT} cells (Fig. 3C–E), as observed in the CAPAN1 coculture model.

Darwinian selection of secondary mutant tumor cells also operates *in vivo*

We also assessed whether a Darwinian process influenced the *in vivo* response to PARPi treatment. To do this, we generated cohorts of mice bearing subcutaneous xenografts consisting of a mixture of CAPAN1 parental and CAPAN1.B2.S* secondary mutant tumor cells (Fig. 4A). We found that inoculating 5×10^6 tumor cells at a 1:1 CAPAN1:CAPAN1.B2.S* ratio reproducibly generated 100 mm³ xenografts 10 days after inoculation, where each clone was present in equal proportion (Fig. 4B). When tumors reached 100 mm³, tumor-bearing mice were randomized into the following treatment cohorts to assess the selective pressure of PARPi treatment *in vivo*: (i) olaparib (50 mg/kg) administered once daily, (ii) olaparib (50 mg/kg) administered every other day, (iii) olaparib (50 mg/kg) administered twice a week on days 1 and 4, (iv) drug vehicle administered daily. In addition, sentinel mice were sacrificed prior to treatment so that the CAPAN1:CAPAN1.B2.S* ratio in tumors prior to therapy could be confirmed (Fig. 4A; Supplementary Fig. S6A). We found that 50 mg/kg olaparib treatment, administered daily, every other day, or twice weekly, though well-tolerated, did not decrease tumor growth compared with the vehicle ($P > 0.05$ ANOVA for tumor volume in each olaparib treatment cohort versus vehicle; Supplementary Fig. S6B and S6C). We hypothesized that the absence of overall antitumor efficacy in this particular case might be due to failure to inhibit the PARPi secondary mutant clone in xenografts. To test this, we

isolated tumor DNA from olaparib-treated mice (after 28-day treatment) and assessed the relative ratio of parental versus secondary mutant clones by ddPCR. In mice that received drug vehicle alone, the ratio of parental versus secondary mutant clones remained approximately 50% (Supplementary Fig. S6A). However, in mice that received olaparib treatment, the relative frequency of CAPAN1.B2.S* cells increased in response to therapy (Fig. 4C). This increase in CAPAN1.B2.S* frequency, in preference to the parental clone, was dependent upon the periodicity of PARPi administration, for example, daily administration of olaparib caused the greatest increase in CAPAN1.B2.S* enrichment, followed by every other day treatment and then biweekly administration (Fig. 4C and D). This suggested that PARPi administration also selected for secondary mutant tumor cell clones *in vivo* and that the degree of secondary mutant clone selection was related to the extent of selective pressure applied.

AZD-1775, a WEE1 kinase inhibitor, targets both parental and secondary *BRCA*-mutant clones *in vitro* and *in vivo*

The coculture model systems described above allowed us to establish that PARPi resistance, when driven by secondary mutations in *BRCA1* or *BRCA2*, can operate along Darwinian principles. We also assessed whether we could identify therapeutic vulnerabilities that would allow targeting of both parental and secondary mutant tumor cell clones as a means to minimize the impact of secondary mutation. We assessed whether small-molecule WEE1 cell-cycle checkpoint kinase inhibitors (WEE1i; ref. 19) might have utility in this regard. We focused on WEE1 inhibitors for a number of reasons. WEE1 prevents premature mitotic entry by phosphorylating and inhibiting cyclin-dependent kinases such as cyclin dependent kinase 1 (CDK1; refs. 31, 32). This activity is particularly critical in tumor cells with p53 pathway defects; p53 defects often cooccur with *BRCA* mutations, and although secondary mutations in *BRCA1/2* drive PARPi resistance, resistant tumors and cell lines remain p53 mutant (13). CAPAN1.B2.S* and SUM149.B1.S* clones retained the p53 mutations present in CAPAN1 and SUM149 parental tumor cell clones (Supplementary Figs. S7 and S8). We also found that in an analysis of *in vitro* sensitivity to the clinical WEE1 kinase inhibitor, AZD-1775, in a panel of tumor cell lines, CAPAN1.B2.S* and SUM149.B1.S* were among the most sensitive of 146 lines profiled (Fig. 5A). We confirmed this AZD-1775 sensitivity in subsequent clonogenic survival experiments and found that, when compared with nontumor breast epithelial cell lines (MCF10A and MCF12A), both CAPAN1 and SUM149-derived secondary mutant tumor cell clones retained profound sensitivity to AZD-1775 seen in parental tumor cells (average 22-fold

(Continued.) the increase in secondary mutant clone frequency following 14 days of drug exposure. **D**, Graph showing the frequency of CAPAN1B2.S* cells in CAPAN1/CAPAN1B2* cocultures exposed to AZD-1775. Clone frequency was estimated by ddPCR and the time points shown. Error bars represent SEM from three independent measurements. This experiment was conducted alongside the experiment described in Fig. 2D; to allow comparison, the response to olaparib, and DMSO exposure from Fig. 2D is replotted here. **E**, Western blot analysis for CAPAN1 and CAPAN1.B2.S* cells lysates probed for pCDC2(Y15), γ -H2AX (a DNA damage marker), and cleaved PARP1 (a marker of apoptosis). Tubulin was used as a loading control. **F**, Experimental schematic of mixed CAPAN1:CAPAN1.B2.S* xenografts treated with olaparib or AZD-1775. **G**, Bar chart illustrating CAPAN-1 (white) to CAPAN-1.B2.S* (red) clone ratio in in tumour xenografts prior to drug treatment. Values shown from six sentinel animals with mean \pm SEM shown. **H**, Tumor volume plotted against length of treatment for individual xenografts comprised of CAPAN1:CAPAN1.B2.S* mixed tumor cells over 150 days ($n = 18$ total, $n = 6$ in each cohort). **I**, Survival curves using maximum tumor size (1,500 mm³) as a surrogate for survival from the experiment shown in **E**. **J**, Bar chart showing proportion of CAPAN1.B2.S* tumor cells following treatment from the experiment shown in **E** ($n = 6$, mean \pm SEM). P values were calculated by Student t test.

difference in AUC, $P < 0.0001$ vs. MCF10A or MCF12A, ANOVA; Fig. 5B). We confirmed these observations using coculture systems and found that at SF₅₀ concentrations (concentration required to inhibit 50% of cells) of either olaparib or AZD-1775, olaparib exposure increased the relative frequency of the secondary mutant clones, but AZD-1775 did not (Fig. 5C). This observation was confirmed when we used ddPCR to monitor the frequency of the secondary mutant clone over time in cocultures exposed to AZD-1775 (Fig. 5D). We also observed that parental and secondary mutant SUM149 and CAPAN1 clones were sensitive to additional small-molecule cell-cycle checkpoint inhibitors including PF-477736, a CHK1 inhibitor (33, 34), and VX-970, an ATR inhibitor (35) when compared with nontumor epithelial cells (Supplementary Fig. S9A and S9B). This suggested that even when partial BRCA1 or BRCA2 protein function was restored by secondary mutation, vulnerability to small-molecule inhibitors that target cell-cycle checkpoints still existed. These effects did not appear to represent a relatively nonspecific sensitivity to cytotoxic agents in the parental and secondary mutant tumor cells, as these did not display an overtly distinct level of sensitivity to paclitaxel, capecitabine, or gemcitabine when compared with MCF10 or MCF12A cells (Supplementary Fig. S9C–S9F).

Previous studies have shown that WEE1 inhibitors cause tumor cell cytotoxicity by reducing the extent of CDC2 phosphorylation at Y15 (36). We found that in both CAPAN1 and CAPAN1.B2.S* cells, AZD-1775 exposure caused a decrease in CDC2 Y15 phosphorylation, an effect that was enhanced with prolonged drug exposure (Fig. 5E). We noted that AZD-1775 exposure caused an increase in H2AX phosphorylation (γ H2AX), a biomarker of DNA damage, in both CAPAN1 and secondary mutant CAPAN1.B2.S* cells (Fig. 5E). This increase in γ H2AX was commensurate with an increase in PARP cleavage, a measure of apoptosis (Fig. 5E). Using FACS profiling, we found that AZD-1775 exposure had a very similar effect on cell-cycle fractions in both CAPAN1 and CAPAN1.B2.S* cells, both of which demonstrated a profound reduction in the fraction of cells in active S-phase, with a commensurate increase in the proportion of cells in nonreplicating S phase (Supplementary Fig. S10). In CAPAN1 cells, AZD-1775 exposure caused a reduction in the active S-phase fraction from 25.9% to 3.4% (with a 3.9%–52.1% increase in nonreplicating S-phase), while CAPAN1.B2.S* cells showed a reduction in active S-phase from 27.8% to 4.2% (with a 3.3%–51.4% increase in nonreplicating S-phase). These observations were reminiscent of those seen in H3K36me3-deficient cells, where WEE1 inhibition also caused a severe reduction in the active S-phase fraction (37). This suggested that WEE1 inhibition targeted CAPAN1 cells in S-phase, regardless of whether BRCA2 was dysfunctional (as in CAPAN1) or somewhat reconstituted by the presence of a secondary BRCA2 mutation (as in CAPAN1.B2.S*).

To investigate whether WEE1 inhibitor sensitivity in PARPi-sensitive and resistant clones also operated *in vivo*, we assessed the effect of AZD-1775 treatment on mice bearing mixed CAPAN1/CAPAN1.B2.S* xenografts (each clone present at a 1:1 ratio, Fig. 5F). Mice with established tumors were treated with either AZD-1775, olaparib, or drug vehicle. Sentinel mice sacrificed prior to treatment showed the CAPAN1:CAPAN1.B2.S* ratio in tumors prior to therapy was 1:1 (Fig. 5G). We used the time taken for tumors to reach 1,500 mm³ as a surrogate measure of survival (Fig. 5H) and found that while olaparib treatment had minimal benefit ($P = 0.86$, log-rank Mantel–Cox test compared with

vehicle), AZD-1775 treatment led to a significant survival benefit ($P = 0.011$, log-rank Mantel–Cox test compared with olaparib; Fig. 5I). Consistent with these observations, ddPCR analysis of tumors at the end of treatment showed that olaparib therapy caused a relative enrichment in the frequency of the secondary mutant clone ($P = 0.058$ compared with vehicle, Student *t* test) while AZD-1775 did not ($P = 0.43$, compared with vehicle, Student *t* test; Fig. 5J).

Discussion

In this study, we used CRISPR-generated BRCA1 or BRCA2 secondary mutant daughter clones alongside isogenic parental cell lines to demonstrate that PARPi exposure selects for secondary mutant clones in a Darwinian manner, both *in vitro* and *in vivo*. We found that the extent of selection for secondary mutant clones was influenced by the frequency of drug administration. In mice bearing tumors comprised of an equal proportion of BRCA2-mutant and BRCA2 secondary mutant tumor cells, olaparib had minimal effects on tumor growth, but did preferentially select for the secondary mutant daughter clone over the parental tumor cell. It would be reasonable to infer that high frequencies of secondary mutant cells hinder the therapeutic effectiveness of PARP inhibitors. We also found that a WEE1 inhibitor, AZD-1775, had a greater therapeutic effect on mixed parental/secondary mutant tumors than olaparib. This example suggests that therapeutic vulnerabilities might still exist in tumors that have a high frequency of secondary mutant clones. Our data also suggest that secondary mutant and parental tumor cells also show sensitivity to other cell cycle/DNA damage repair inhibitors, including CHK1 and ATR inhibitors (Supplementary Fig. S9). It seems possible that while secondary BRCA1 or BRCA2 gene mutations restore some HR function, these are unlikely to reverse the complex set of genomic rearrangements, aneuploidy, and p53 mutations found in BRCA1 or BRCA2 mutant tumors prior to treatment (38). We hypothesize that these latter characteristics sensitize tumor cells to drugs such as WEE1 inhibitors, perhaps explaining why AZD-1775 targets both parental and secondary mutant clones. This hypothesis remains to be tested, but the observation that secondary mutant tumor cells are sensitive to AZD-1775 raises the possibility that therapeutic vulnerabilities still exist in PARPi-resistant tumors.

In clinical studies, the MTD for single-agent AZD-1775 was identified as 225 mg twice per day orally over 2.5 days per week for 2 weeks per 21-day cycle, a dosing regimen sufficient to elicit a number of antitumor responses (39). In our *in vivo* studies (Fig. 5) we used 30 mg/kg AZD-1775 twice-daily treatments for the entire duration of the study (150 days). This treatment approach was well tolerated in mice and based on prior mouse-based experiments using this WEE1 inhibitor (40). Nevertheless, it is possible that a similar constant dosing approach may not be well-tolerated in humans. Subsequent work might assess the potential of using intermittent WEE1 inhibitor dosing schedules to assess whether these also elicit a survival benefit in experiments similar to those shown in Fig. 5.

One implication of this work is that the detection of secondary BRCA1 or BRCA2 mutations in patients could be important in influencing the choice of therapy. At present, secondary mutations in BRCA1 or BRCA2 can be detected by Sanger DNA sequencing (14–16) or by targeted DNA capture and deep sequencing (13). Circulating tumor DNA and circulating tumor cells might also

display some of the secondary *BRCA1* or *BRCA2* mutations found in solid tumors. Detecting secondary mutations in such liquid biopsies might allow the early emergence of secondary mutations to be identified as a biomarker predicting the eventual clinical manifestation of PARPi resistance. One avenue we will now explore is to utilize the *in vivo* system we have described here to assess this possibility. A key quality of the model systems described here is that they allow the construction of cocultures and xenografts where the frequency and identity of secondary mutants is known. This will hopefully facilitate experiments that aim to examine further principles that govern clonal evolution and influence drug resistance in *BRCA1*- or *BRCA2*-mutant cancers. Alongside these models, we also note that the first PDX with PARPi resistance-causing mutations have been recently described (41). These provide another system in which to assess how the clonal structure of tumors evolve in response to therapy. The combined use of engineered systems, such as that described here, alongside PDX systems will be critical in establishing what factors determine the response to treatment, and importantly, what therapeutic approaches could be taken to minimize the impact of secondary *BRCA1/2* gene mutations.

Disclosure of Potential Conflicts of Interest

N.C. Turner reports receiving commercial research support from AstraZeneca and is a consultant/advisory board member for AstraZeneca. A. Ashworth provided expert testimony for AstraZeneca. C.J. Lord has received speakers bureau honoraria from AstraZeneca and Vertex and is a consultant/advisory board member for Vertex and Sun Pharma. A. Ashworth and C.J. Lord are named inventors on patents describing the use of PARP inhibitors and stand to gain from their use as part of the ICR "Rewards to Inventors" scheme. No potential conflicts of interest were disclosed by the other authors.

References

- Domchek SM, Armstrong K, Weber BL. Clinical management of *BRCA1* and *BRCA2* mutation carriers. *Nat Clin Pract Oncol* 2006;3:2–3.
- Alexandrov LB, Nik-Zainal S, Wedge DC, Aparicio SA, Behjati S, Biankin AV, et al. Signatures of mutational processes in human cancer. *Nature* 2013;500:415–21.
- Tutt A, Bertwistle D, Valentine J, Gabriel A, Swift S, Ross G, et al. Mutation in *Brca2* stimulates error-prone homology-directed repair of DNA double-strand breaks occurring between repeated sequences. *EMBO J* 2001;20:4704–16.
- Moynahan ME, Chiu JW, Koller BH, Jasin M. *Brca1* controls homology-directed DNA repair. *Mol Cell* 1999;4:511–8.
- Johnson RD, Liu N, Jasin M. Mammalian *XRCC2* promotes the repair of DNA double-strand breaks by homologous recombination. *Nature* 1999;401:397–9.
- Arnaudeau C, Lundin C, Helleday T. DNA double-strand breaks associated with replication forks are predominantly repaired by homologous recombination involving an exchange mechanism in mammalian cells. *J Mol Biol* 2001;307:1235–45.
- Lord CJ, Tutt AN, Ashworth A. Synthetic lethality and cancer therapy: lessons learned from the development of PARP inhibitors. *Annu Rev Med* 2015;66:455–70.
- Ledermann J, Harter P, Gourley C, Friedlander M, Vergote I, Rustin G, et al. Olaparib maintenance therapy in patients with platinum-sensitive relapsed serous ovarian cancer: a preplanned retrospective analysis of outcomes by *BRCA* status in a randomised phase 2 trial. *Lancet Oncol* 2014;15:852–61.
- Ledermann J, Harter P, Gourley C, Friedlander M, Vergote I, Rustin G, et al. Olaparib maintenance therapy in platinum-sensitive relapsed ovarian cancer. *N Engl J Med* 2012;366:1382–92.
- Audeh MW, Carmichael J, Penson RT, Friedlander M, Powell B, Bell-McGuinn KM, et al. Oral poly(ADP-ribose) polymerase inhibitor olaparib in patients with *BRCA1* or *BRCA2* mutations and recurrent ovarian cancer: a proof-of-concept trial. *Lancet* 2010;376:245–51.
- Tutt A, Robson M, Garber JE, Domchek SM, Audeh MW, Weitzel JN, et al. Oral poly(ADP-ribose) polymerase inhibitor olaparib in patients with *BRCA1* or *BRCA2* mutations and advanced breast cancer: a proof-of-concept trial. *Lancet* 2010;376:235–44.
- Lord CJ, Ashworth A. Mechanisms of resistance to therapies targeting *BRCA*-mutant cancers. *Nat Med* 2013;19:1381–8.
- Barber LJ, Sandhu S, Chen L, Campbell J, Kozarewa I, Fenwick K, et al. Secondary mutations in *BRCA2* associated with clinical resistance to a PARP inhibitor. *J Pathol* 2013;229:422–9.
- Norquist B, Wurz KA, Pennil CC, Garcia R, Gross J, Sakai W, et al. Secondary somatic mutations restoring *BRCA1/2* predict chemotherapy resistance in hereditary ovarian carcinomas. *J Clin Oncol* 2011;29:3008–15.
- Edwards SL, Brough R, Lord CJ, Natrajan R, Vatcheva R, Levine DA, et al. Resistance to therapy caused by intragenic deletion in *BRCA2*. *Nature* 2008;451:1111–5.
- Sakai W, Swisher EM, Jacquemont C, Chandramohan KV, Couch FJ, Langdon SP, et al. Functional restoration of *BRCA2* protein by secondary *BRCA2* mutations in *BRCA2*-mutated ovarian carcinoma. *Cancer Res* 2009;69:6381–6.
- Greaves M, Maley CC. Clonal evolution in cancer. *Nature* 2012;481:306–13.
- Issaeva N, Thomas HD, Djureinovic T, Jaspers JE, Stoimenov I, Kyle S, et al. 6-thioguanine selectively kills *BRCA2*-defective tumors and overcomes PARP inhibitor resistance. *Cancer Res* 2010;70:6268–76.
- Hirai H, Iwasawa Y, Okada M, Arai T, Nishibata T, Kobayashi M, et al. Small-molecule inhibition of Wee1 kinase by MK-1775 selectively sensitizes p53-deficient tumor cells to DNA-damaging agents. *Mol Cancer Ther* 2009;8:2992–3000.
- Shen Y, Rehman FL, Feng Y, Boshuizen J, Bajrami I, Elliott R, et al. BMN 673, a novel and highly potent PARP1/2 inhibitor for the treatment of human cancers with DNA repair deficiency. *Clin Cancer Res* 2013;19:5003–15.

Authors' Contributions

Conception and design: A. Dréan, C.T. Williamson, A. Ashworth, C.J. Lord
Development of methodology: A. Dréan, C.T. Williamson, I. Garcia-Murillas, C.J. Lord
Acquisition of data (provided animals, acquired and managed patients, provided facilities, etc.): A. Dréan, R. Brough, I. Brandsma, M. Menon, A. Konde, H.N. Pemberton, J. Frankum, N. Badham, C.J. Lord
Analysis and interpretation of data (e.g., statistical analysis, biostatistics, computational analysis): A. Dréan, C.T. Williamson, A. Konde, I. Garcia-Murillas, H.N. Pemberton, J. Campbell, A. Gulati, N.C. Turner, C.J. Lord
Writing, review, and/or revision of the manuscript: A. Dréan, C.T. Williamson, N.C. Turner, S.J. Pettitt, A. Ashworth, C.J. Lord
Administrative, technical, or material support (i.e., reporting or organizing data, constructing databases): M. Menon, A. Konde, R. Rafiq, C.J. Lord
Study supervision: C.T. Williamson, A. Ashworth, C.J. Lord

Acknowledgments

This work was funded by Breast Cancer Now and Cancer Research UK as part of Programme Grants (to C.J. Lord). We thank the Tumour Profiling Unit (TPU) at the Institute of Cancer Research for carrying out DNA sequence analysis. We acknowledge NIHR funding to the Royal Marsden Biomedical Research Centre.

Grant Support

This work was supported by Breast Cancer Now (CTR-Q4-Y2; to C.J. Lord) and Cancer Research UK (CRUK/A14276; to C.J. Lord).

The costs of publication of this article were defrayed in part by the payment of page charges. This article must therefore be hereby marked *advertisement* in accordance with 18 U.S.C. Section 1734 solely to indicate this fact.

Received January 30, 2017; revised May 2, 2017; accepted June 5, 2017; published OnlineFirst June 15, 2017.

Dréan et al.

21. Hill SJ, Clark AP, Silver DP, Livingston DM. BRCA1 pathway function in basal-like breast cancer cells. *Mol Cell Biol* 2014;34:3828–42.
22. Miller RE, Brough R, Bajrami I, Williamson CT, McDade S, Campbell J, et al. Synthetic lethal targeting of ARID1A-mutant ovarian clear cell tumors with dasatinib. *Mol Cancer Ther* 2016;15:1472–84.
23. Farmer H, McCabe N, Lord CJ, Tutt AN, Johnson DA, Richardson TB, et al. Targeting the DNA repair defect in BRCA mutant cells as a therapeutic strategy. *Nature* 2005;434:917–21.
24. Pender A, Garcia-Murillas I, Rana S, Cutts RJ, Kelly G, Fenwick K, et al. Efficient genotyping of KRAS mutant non-small cell lung cancer using a multiplexed droplet digital PCR approach. *PLoS One* 2015;10:e0139074.
25. Campbell J, Ryan CJ, Brough R, Bajrami I, Pemberton HN, Chong IY, et al. Large-scale profiling of kinase dependencies in cancer cell lines. *Cell Reports* 2016;14:2490–501.
26. Goggins M, Schutte M, Lu J, Moskaluk CA, Weinstein CL, Petersen GM, et al. Germline BRCA2 gene mutations in patients with apparently sporadic pancreatic carcinomas. *Cancer Res* 1996;56:5360–4.
27. Elstrodt F, Hollestelle A, Nagel JH, Gorin M, Wasielewski M, van den Ouweland A, et al. BRCA1 mutation analysis of 41 human breast cancer cell lines reveals three new deleterious mutants. *Cancer Res* 2006;66:41–5.
28. Hindson CM, Chevillet JR, Briggs HA, Gallichotte EN, Ruf IK, Hindson BJ, et al. Absolute quantification by droplet digital PCR versus analog real-time PCR. *Nat Methods* 2013;10:1003–5.
29. Hudt T, Rago C, Gallmeier E, Brody JR, Gorospe M, Kern SE. A syngeneic variance library for functional annotation of human variation: application to BRCA2. *Cancer Res* 2008;68:5023–30.
30. Zimmer J, Tacconi EM, Folio C, Badie S, Porru M, Klare K, et al. Targeting BRCA1 and BRCA2 deficiencies with G-quadruplex-interacting compounds. *Mol Cell* 2016;61:449–60.
31. Molinari M. Cell cycle checkpoints and their inactivation in human cancer. *Cell Prolif* 2000;33:261–74.
32. Liu Q, Guntuku S, Cui XS, Matsuoka S, Cortez D, Tamai K, et al. Chk1 is an essential kinase that is regulated by Atr and required for the G(2)/M DNA damage checkpoint. *Genes Dev* 2000;14:1448–59.
33. Blasina A, Hallin J, Chen E, Arango ME, Kraynov E, Register J, et al. Breaching the DNA damage checkpoint via PF-00477736, a novel small-molecule inhibitor of checkpoint kinase 1. *Mol Cancer Ther* 2008;7:2394–404.
34. Ashwell S, Janetka JW, Zabludoff S. Keeping checkpoint kinases in line: new selective inhibitors in clinical trials. *Expert Opin Investig Drugs* 2008;17:1331–40.
35. Hall AB, Newsome D, Wang Y, Boucher DM, Eustace B, Gu Y, et al. Potentiation of tumor responses to DNA damaging therapy by the selective ATR inhibitor VX-970. *Oncotarget* 2014;5:5674–85.
36. Do K, Doroshov JH, Kummar S. Wee1 kinase as a target for cancer therapy. *Cell Cycle* 2013;12:3159–64.
37. Pfister SX, Markkanen E, Jiang Y, Sarkar S, Woodcock M, Orlando G, et al. Inhibiting WEE1 selectively kills histone H3K36me3-deficient cancers by dNTP starvation. *Cancer Cell* 2015;28:557–68.
38. Nik-Zainal S, Davies H, Staaf J, Ramakrishna M, Glodzik D, Zou X, et al. Landscape of somatic mutations in 560 breast cancer whole-genome sequences. *Nature* 2016;534:47–54.
39. Do K, Wilsker D, Ji J, Zlott J, Freshwater T, Kinders RJ, et al. Phase I study of single-agent AZD1775 (MK-1775), a Wee1 kinase inhibitor, in patients with refractory solid tumors. *J Clin Oncol* 2015;33:3409–15.
40. Aarts M, Sharpe R, Garcia-Murillas I, Gevensleben H, Hurd MS, Shumway SD, et al. Forced mitotic entry of S-phase cells as a therapeutic strategy induced by inhibition of WEE1. *Cancer Discov* 2012;2:524–39.
41. Ter Brugge P, Kristel P, van der Burg E, Boon U, de Maaker M, Lips E, et al. Mechanisms of therapy resistance in patient-derived xenograft models of BRCA1-deficient breast cancer. *J Natl Cancer Inst* 2016;108:djw148.

Molecular Cancer Therapeutics

Modeling Therapy Resistance in *BRCA1/2*-Mutant Cancers

Amy Dréan, Chris T. Williamson, Rachel Brough, et al.

Mol Cancer Ther 2017;16:2022-2034. Published OnlineFirst June 15, 2017.

Updated version Access the most recent version of this article at:
[doi:10.1158/1535-7163.MCT-17-0098](https://doi.org/10.1158/1535-7163.MCT-17-0098)

Supplementary Material Access the most recent supplemental material at:
<http://mct.aacrjournals.org/content/suppl/2017/06/15/1535-7163.MCT-17-0098.DC1>

Cited articles This article cites 40 articles, 15 of which you can access for free at:
<http://mct.aacrjournals.org/content/16/9/2022.full#ref-list-1>

Citing articles This article has been cited by 3 HighWire-hosted articles. Access the articles at:
<http://mct.aacrjournals.org/content/16/9/2022.full#related-urls>

E-mail alerts [Sign up to receive free email-alerts](#) related to this article or journal.

Reprints and Subscriptions To order reprints of this article or to subscribe to the journal, contact the AACR Publications Department at pubs@aacr.org.

Permissions To request permission to re-use all or part of this article, use this link
<http://mct.aacrjournals.org/content/16/9/2022>.
Click on "Request Permissions" which will take you to the Copyright Clearance Center's (CCC) Rightslink site.